

# An alternative flat scanner and micropositioning method for scanning probe microscope

Wei Cai, Guangyi Shang,<sup>a)</sup> Yusheng Zhou, Ping Xu, and Junen Yao

*Department of Applied Physics, Beihang University, Beijing 100191, People's Republic of China and Key Laboratory of Micro-nano Measurement-Manipulation and Physics (Ministry of Education), Beihang University, Beijing 100191, People's Republic of China*

(Received 29 April 2010; accepted 5 October 2010; published online 8 December 2010)

An alternative flat scanner used for combining a scanning probe microscope with an inverted optical microscope is presented. The scanner has a novel structure basically consisting of eight identical piezoelectric tubes, metal flexure beams, and one sample mount. Because of the specially designed structure, the scanner is able to carry a sample of more than 120 g during imaging. By applying voltages of  $\pm 150$  V, scanning range of more than  $30\ \mu\text{m}$  in three dimensions can be achieved. To improve the reliability of the stick-slip motion, a new method for sample micropositioning is proposed by applying a pulsed voltage to the piezotubes to produce a motion in the  $z$ -axis. Reliable translation of the sample has been thus accomplished with the step length from  $\sim 700$  nm to  $9\ \mu\text{m}$  over a range of several millimeters. A homemade scanning probe microscope–inverted optical microscope system based on the scanner is described. Experimental results obtained with the system are shown. © 2010 American Institute of Physics. [doi:10.1063/1.3505781]

## I. INTRODUCTION

Scanning probe microscope (SPM) has been an important tool for research in nanoscience and nanotechnology.<sup>1–3</sup> By scanning a tip/sample and sensing local tip-sample interactions, SPM is able to produce images of structure and property of a sample surface with nanometer-scale to atomic resolution.<sup>4,5</sup> Critical techniques for SPM are the realization of tip/sample scanning in the  $x$ - $y$  plane and tip-sample distance control in the  $z$ -axis. A number of scanning methods have been developed including piezoelectric tripod scanner, single tube scanner, and a cross-shaped piezoelectric element combined with a single tube.<sup>6</sup> The most successfully used and commercially available SPMs utilize the piezoelectric single tube scanner, first proposed by Binnig and Smith.<sup>7</sup> In their design, the outer electrode of the tube is divided into four equal quadrants while the inside electrode is not separated. One end of the tube is fixed and the other end is free. By applying voltages to four quadrants and inside electrodes, the tube provides three-dimensional motions in  $x$ - $y$ - $z$  directions. The advantages of the tube scanner are simple, compact, and low cost to manufacture. Recently, it has been reported that performance of the tube scanner, such as the positioning accuracy and the bandwidth, can be further improved by using model-based control and estimation techniques.<sup>8</sup> As Lieberman *et al.* pointed out, however, the main drawback of the tube scanner is the large axial size, resulting in a major problem with the combination of SPM and an optical microscope. They have developed a flat scanner based on four piezoelectric tubes and built a fully integrated near-field optical, far-field optical, and normal-force scanned probe microscope.<sup>9</sup> Their work introduces a new way, based on which several instruments can be easily integrated.

The micropositioning over a very large range (several millimeters) is also a key technique in SPM for searching an interest area of the sample or for approaching the tip to the sample surface. Since the original micropositioning device or “louse” was first built by Binnig *et al.*,<sup>2,10</sup> many micropositioning devices have been developed based on the piezoelectric effect.<sup>11–17</sup> Among them, the inertial stick-slip motion first described by Pohl<sup>11</sup> has been widely used. Based on the principle, sample translation can be easily accomplished when the sample is mounted on the free end of the single tube scanner or on the flat scanner. As reported in the literature,<sup>13</sup> however, the disadvantage of inertial stick-slip motion is that the sample movement is unreliable when a driving voltage of a sawtooth waveform is used.

In this paper, we present an alternative flat scanner used for combining a SPM with an inverted optical microscope (IOM). The scanner has a novel structure basically consisting of eight identical piezoelectric tubes, metal flexure beams, and one sample mount. Because of the specially designed structure, the scanner is able to carry a sample of more than 120 g during SPM operation, which will be useful for mounting an accessory on the scanner, such as a magnetic or a heating device. By applying voltages of  $\pm 150$  V, scanning range of more than  $30\ \mu\text{m}$  in three dimensions can be achieved. A new method for sample micropositioning by applying a pulsed voltage to the piezotubes to produce a motion in the  $z$ -axis is demonstrated. A homemade SPM equipped with the flat scanner and combined with an IOM is described. Experimental results obtained with the scanning probe microscope–inverted optical microscope (SPM–IOM) system will be shown.

## II. DESIGN

### A. Mechanical design

Figure 1 shows the schematic structure of our flat scanner, which basically consists of one aluminum frame ( $F$ ),

<sup>a)</sup> Author to whom correspondence should be addressed. Electronic mail: gyshang@buaa.edu.cn.

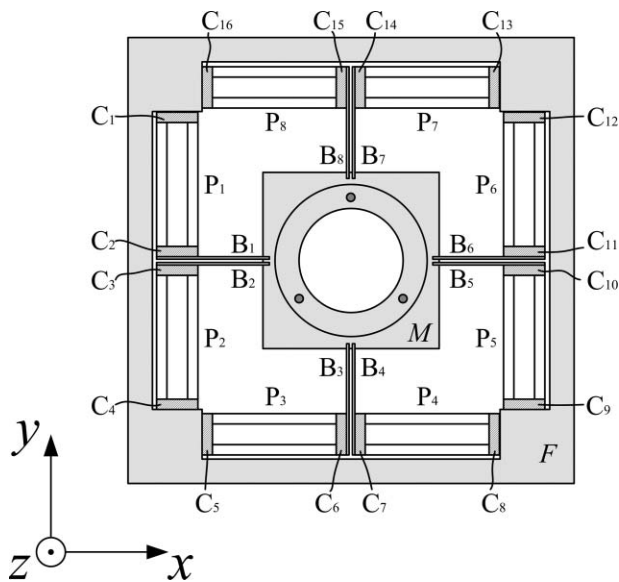


FIG. 1. Schematic structure of the flat scanner, which basically consists of one aluminum frame ( $F$ ), eight piezoelectric tubes ( $P_1$ – $P_8$ ), eight copper flexible beams ( $B_1$ – $B_8$ ), and one aluminum sample mount ( $M$ ) with a 30 mm diameter aperture at its center. Sixteen ceramic plates ( $C_1$ – $C_{16}$ ) were used for electric isolation between the frame/beams and piezotube electrodes.

eight piezoelectric tubes ( $P_1$ – $P_8$ ), eight copper flexible beams ( $B_1$ – $B_8$ ), and one aluminum sample mount ( $M$ ) with a 30 mm diameter aperture at its center. Three steel balls with diameter of 3 mm were arranged on the sample mount for supporting a sample.

The scanner was fabricated by gluing one end of the tube  $P_i$  to that of the flexible beam  $B_i$  and then attaching the other end of the tube to the frame. Sixteen ceramic plates ( $C_1$ – $C_{16}$ ) were used for electric isolation between the frame/beams and piezotube electrodes. By being fixed to the other ends of all flexible beams, the sample mount was finally supported by eight piezotube-flexible beam assemblies, completing a piezotube driving and flexible-beam guiding system. By applying appropriate control voltages to the piezotube electrodes, sample scanning in  $x$ - $y$ - $z$  directions and micropositioning in the  $x$ - $y$  plane can be accomplished.

In contrast to the previously reported flat scanner,<sup>9</sup> our design features the symmetric arrangement about the  $x$ - $y$ -axis. Since driving forces produced by the piezotubes are applied to the  $x$ - $y$ -axis of the sample mount via the flexible beams, no angular moments act upon the sample mount. The sample motion along the  $x$ - $y$ -axis is thus accomplished without the trend to rotation. In addition, the design provides a strong structure, allowing the sample mount to take a load of more than 120 g. This capability will be useful for putting an accessory on the scanner, such as a magnetic or a heating device for the study of magnetic materials in our laboratory.

## B. Electrical connection

The piezotubes are made from lead zirconate titanate (PZT-5A) material and have the same dimensions of 35 mm long, 8 mm outer diameter, and 0.6 mm wall thickness. The

outer electrode of each tube is divided into four equal quadrants while the inside electrode is not separated.

The right side electrodes of quadranted piezotube  $P_1$ ,  $P_2$ ,  $P_5$ , and  $P_6$  are connected to a scan voltage  $V_{+X}$ . The left side electrodes of these four tubes are connected to  $V_{-X}$ . The electrodes in the upside face of tube  $P_3$ ,  $P_4$ ,  $P_7$ , and  $P_8$  are connected to  $V_{+Y}$ , and the downside electrodes of these four tubes are connected to  $V_{-Y}$ . All top electrodes of eight tubes are connected to  $V_{+Z}$ , and all bottom electrodes are connected to  $V_{-Z}$ . The inside electrodes of the tubes are grounded.

## III. SCANNING AND MICROPOSITIONING CONTROL

### A. Scanning

By applying scan voltages  $V_{+X}$  and  $V_{-X}$  to the left and right electrodes of the piezotubes ( $P_1$ ,  $P_2$ ,  $P_5$ , and  $P_6$ ) at the same time, the piezotubes together with the flexible beams ( $B_1$ ,  $B_2$ ,  $B_5$ , and  $B_6$ ) will drive the sample mount to scan in the  $x$ -axis. While scan voltages  $V_{+Y}$  and  $V_{-Y}$  are applied to the up and down electrodes of the tubes ( $P_3$ ,  $P_4$ ,  $P_7$ , and  $P_8$ ), the sample mount can move in the  $y$ -axis. As voltages  $V_{+Z}$  and  $V_{-Z}$  are applied to the top and bottom electrodes of each tube, the mount will have a motion in the  $z$ -axis. With typical scan voltages of  $\pm 150$  V, three-dimensional scanning with the range of more than 30  $\mu\text{m}$  has been carried out. The larger scanning range can be achieved by changing the dimensions of the piezotubes. In fact, the scan range of  $\sim 30$   $\mu\text{m}$  is adequate for SPM that is combined with an IOM.

### B. Micropositioning

To produce a sample translation based on the stick-slip effect, a sawtooth waveform driving voltage is used in our experiment. In principle, when voltages applied to the piezotubes ( $P_1$ ,  $P_2$ ,  $P_5$ , and  $P_6$ ) are slowly increased, the sample mount will move to right, making the sample move at the same time due to the static friction force. The rapid jump of the voltages makes the mount come back to its initial position immediately. In this case, the sample remains stationary due to inertia, resulting in a net displacement. By repeating this process, continuous motion of the sample is carried out in the  $x$ -axis. Similarly, motion of the sample in the  $y$ -axis can be also produced by applying driving voltages to the piezotubes ( $P_3$ ,  $P_4$ ,  $P_7$ , and  $P_8$ ). As reported in the literature,<sup>13</sup> however, we also found that the sample movement was unreliable in the step-by-step motion in our experiment.

The stick-slip effect has been extensively studied by using computer simulation and experimental method.<sup>18–20</sup> The studies give the simple conclusion that properly controlling the inertial force and the friction force is an important issue, which strongly influence the performance of a micropositioner. Obviously, it is easy to make the inertial force to be smaller than the static friction force by slowly increasing driving voltages. The major problem to be considered here is how to properly control the inertial force to exceed the friction force. To meet this condition, an alternative way is the reduction of the friction force. We thus propose a method to dramatically reduce the friction force by applying a minus

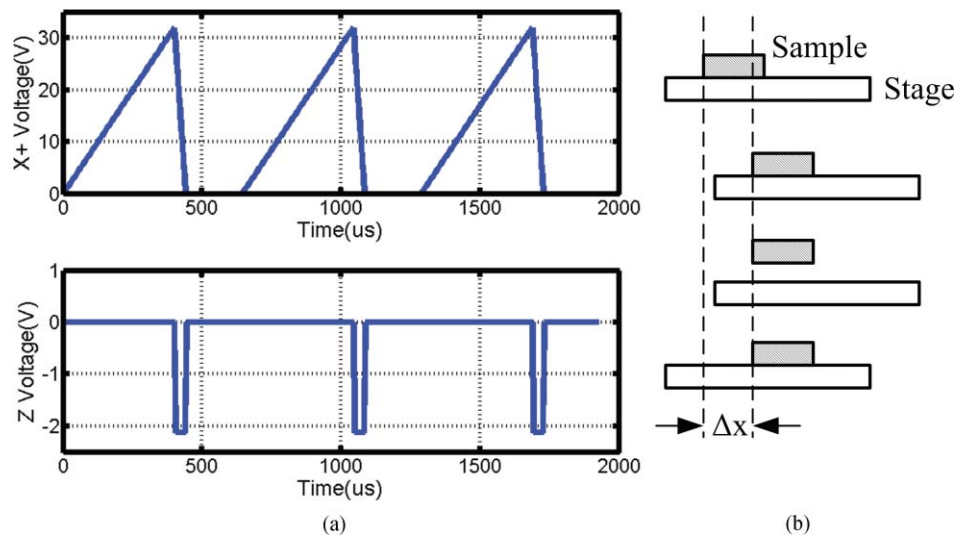


FIG. 2. (Color online) (a) The waveforms of the driving and pulsed voltages applied to the scanner simultaneously. (b) Stick-separation-slip procedures in one step of the sample motion.

pulsed voltage  $\Delta V$  to the piezotubes to produce a motion in the  $z$ -axis.

Since the piezotube can be treated as a linear component,<sup>11</sup> when the pulsed voltage  $\Delta V$  is applied to one of piezotubes, the impact force  $F_z$  produced by  $\Delta V$  can be written as

$$F_z = E \Delta V \quad (1)$$

and the displacement in the  $z$ -axis  $\Delta z$  is given by

$$\Delta z = D \Delta V, \quad (2)$$

where  $E$  and  $D$  are constants denoting force and expansion per volt, respectively. The force  $F_z$  can also be expressed by

$$F_z = K \Delta z, \quad (3)$$

where  $K$  is the spring constant of the tube in the  $z$ -axis of the scanner. From Eqs. (1)–(3), we have

$$E = K D. \quad (4)$$

The driving and pulsed voltages simultaneously applied to the tubes are given in Fig. 2(a). During the driving voltage decreasing rapidly, the pulsed voltage  $\Delta V$  is applied, making the sample mount come down. In this situation, the acceleration of the sample mount and the sample can be estimated by

$$a = \frac{8F}{m_1 + m_2} = \frac{8KD\Delta V}{m_1 + m_2}, \quad (5)$$

where  $m_1$  and  $m_2$  is the mass of the sample mount and the sample, respectively. It is ideal for operation of sample slipping that the acceleration  $a$  is larger than gravity acceleration  $g$ . Thus we have

$$\Delta V \geq \frac{(m_1 + m_2)g}{8KD}. \quad (6)$$

From Eq. (6), it is easy to know that the pulsed voltage  $\Delta V$  applied to the piezotubes is proportional to the mass of the sample. When  $\Delta V$  is larger than the minimum value of  $\Delta V$ ,

the acceleration of the sample mount will exceed gravity acceleration of the sample. In this case, the sample will be separated from the sample mount, making the friction force between them reduce to zero. Since there is no influence of the friction force, slipping between the sample and sample mount will take place very smoothly. The “stick-separation-slip” procedures in one step motion of the sample are shown in Fig. 2(b).

#### IV. EXPERIMENTAL SETUP AND RESULTS

To test the performance of the flat scanner, a SPM equipped with the flat scanner has been built and mounted on the stage of the IOM (IBE2000, Chongqing Photo-electronic Instrument Inc., People’s Republic of China) with a CCD camera and 50 $\times$  objective. Figure 3 gives a picture of the SPM–IOM system. A commercially available SPM controller (CSPM5000, Benyuan Nano-Instruments Co., People’s

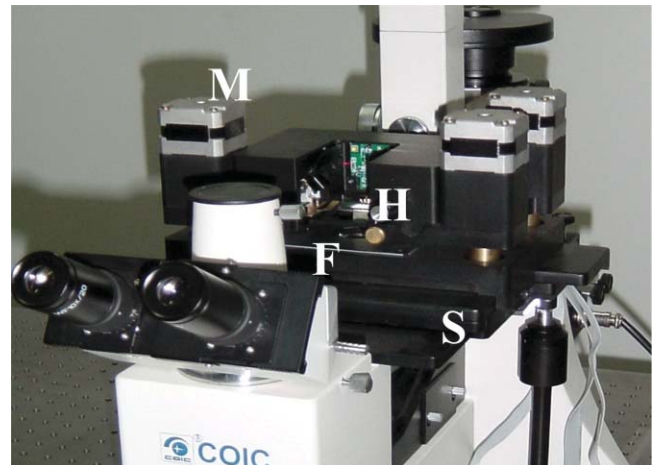


FIG. 3. (Color online) A picture of the SPM–IOM system, which mainly consists of the flat scanner (F), the probe holder (H), the stepping motors (M), and the stage (S) of the optical microscope.

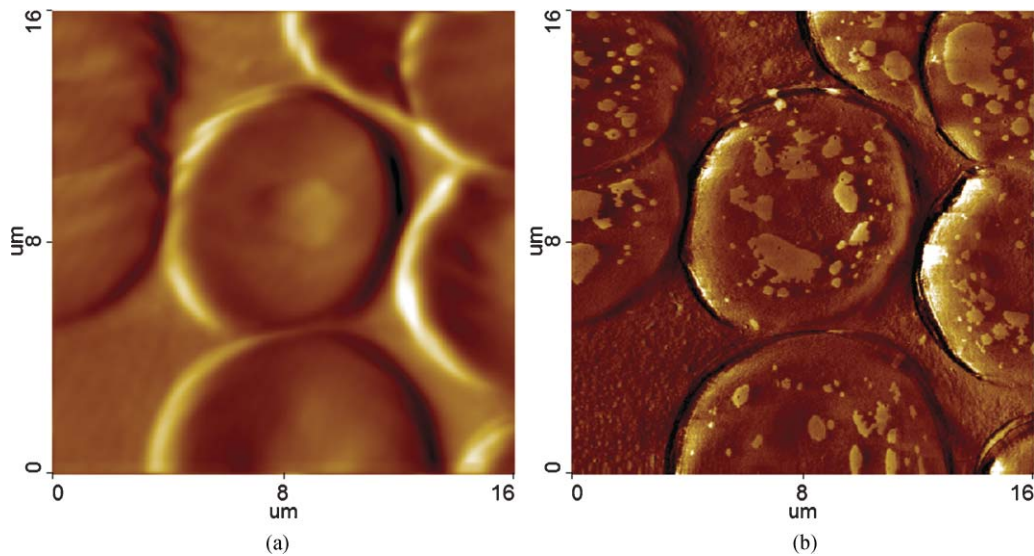


FIG. 4. (Color online) AFM topographic (a) and friction (b) images of red blood cells scanned with the flat scanner.

Republic of China) is used, which has the abilities of signal generation, lock-in measurement,  $x$ - $y$  scan, feedback control, data acquisition, and image display. The SPM-IOM system allows one to take AFM, shear force, near-field optical, and far-field optical images of a sample by changing the probe holder that is specially designed for AFM or scanning near-field optical microscope (SNOM) imaging.<sup>21</sup> Voltages applied to the scanner for micropositioning are generated by a peripheral component interconnect (PCI) multichannel 16-bit digital-to-analog card (PCI7489, Beijing Hotec Control Co., People's Republic of China) and then amplified by high-voltage amplifiers (PA240, Apex Microtechnology, USA).

Using the system, various samples were investigated and typical results of AFM images of red blood cells (RBCs) on glass cover slip are shown in Fig. 4. RBCs have been extensively studied by AFM because of their relatively simple structure and ease of isolation.<sup>22,23</sup> In the presented images, concave shape and some fine structures of the RBCs are clearly observed. The shape and dimension are in agreement with the results previously reported in the literatures.<sup>22,23</sup> In Fig. 5, shear force topographic, amplitude, and near-field

transmission optical images of a test grating (SNG01, NT-MDT, Russia) are given, which were obtained simultaneously at the set-point of  $\sim 0.95$  and the line scan rate of 0.5 Hz. In the topographic image, the rhomb shaped structures and some small particles are clearly presented. In the corresponding transmission image of SNOM, the same rhomb shaped structures are imaged more darkly than other regions. The contrast of the optical image results from more optical absorption of the rhomb shaped metal films than that of the glass substrate. Those results imply that the scanner as well as the system has excellent performance. We also experimentally found that this scanner can carry a sample of more than 120 g weight during SPM imaging.

As a preliminary experiment for our stick-separation-slip method, the relationship between the average step length of the sample motion and the driving voltage was investigated at different pulsed voltages. The experiment was performed by moving the grating sample ( $3 \mu\text{m}$  in the period, TGZ3, NT-MDT, Russia) with the stick-separation-slip method and measuring the average step length with the IOM. To reduce measurement error, 100 data were collected for each point.

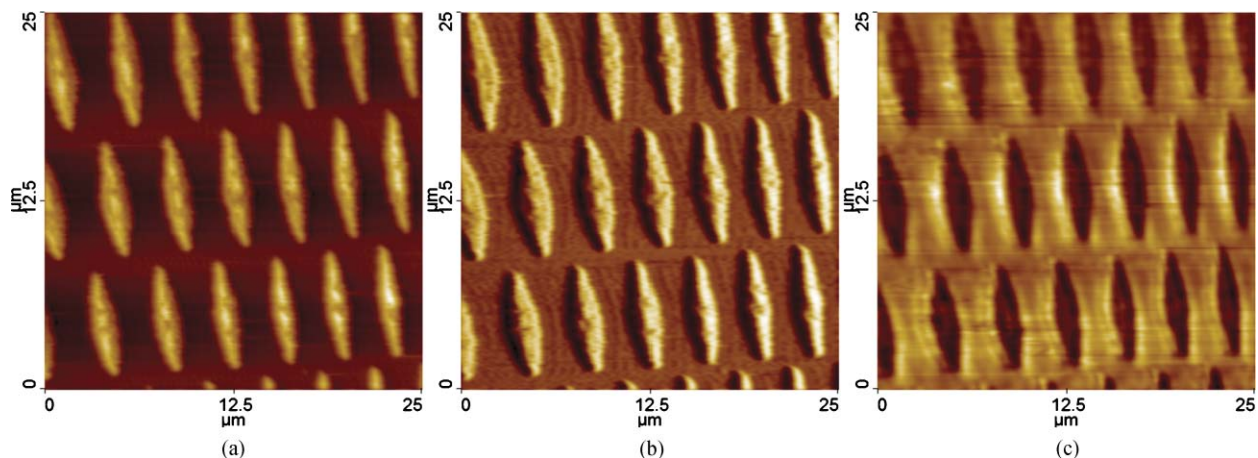


FIG. 5. (Color online) Shear force topographic (a), amplitude (b), and near-field transmission optical (c) images of the test grating obtained simultaneously.

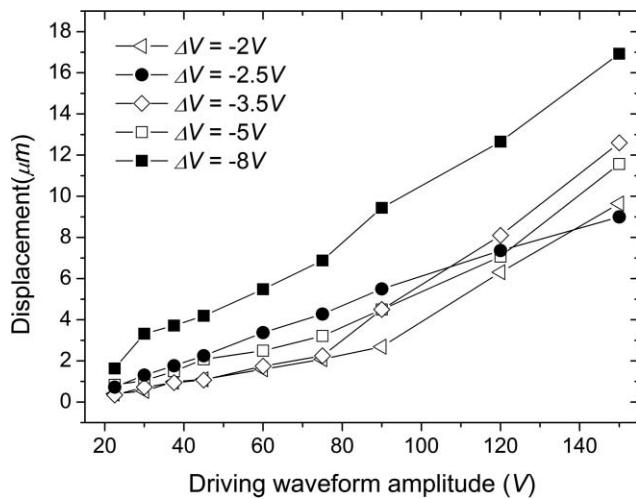


FIG. 6. Experimental curves of the average step length as a function of the driving voltage under the different pulsed voltage  $\Delta V$ . The mass of the sample in the experiment is  $\sim 10$  g.

The experimental results are given in Fig. 6. We found that there was a threshold value of  $\sim 1.5$  V for the pulsed voltage. When the pulsed voltage was smaller than this value, the sample motion became unreliable. This experimental result is in agreement with that we discussed above. We also found that the average step length was affected by the pulsed voltage  $\Delta V$  when the driving voltages were a fixed value. For example, when the driving voltages were 90 V, the average step length was  $\sim 2.7$  and  $9.4$   $\mu\text{m}$  under the condition of  $\Delta V$  being 2.5 and 8 V, respectively. The average step length of the latter is  $\sim 3.5$  times larger than that of the former. This phenomenon could be briefly explained as follows. Since the piezotubes can be treated as linear components, the larger pulsed voltage produces a larger acceleration and a longer displacement, as well as a longer separate time between the sample and sample mount during the slipping phase. Consequently, the increase of the step length with the pulsed voltage takes place even at the fixed driving voltages. From Fig. 6, it is easy to know that when  $\Delta V$  is 2.5 V the relation between the step length and the driving voltage is almost linear. In this condition, reliable stick-separation-slip movement of the sample can be accomplished with the step length from  $\sim 700$  nm to  $9$   $\mu\text{m}$ . The work concerning the simulation and experiment of the stick-separation-slip method will be further done and presented in a separate article.

## V. DISCUSSION

We have developed an alternative flat scanner used for the SPM-IOM system in our laboratory. Compared with the previously reported flat scanner, the feature of our design is the symmetric arrangement about the  $x$ - $y$ -axis. Since driving forces produced by the piezotubes are applied to the  $x$ - $y$ -axis of the sample mount via the flexible beams, no angular moments act upon the sample mount. The sample motion along the  $x$ - $y$ -axis is thus accomplished without the trend to rotation. In addition, the design provides a strong structure,

allowing the sample mount to carry a sample of more than 120 g. This capability will be useful for putting an accessory on the scanner, such as a magnetic or a heat device for the study of magnetic materials in the next work in our laboratory. Based on the scanner, a SPM-IOM system has been successfully built. The results show that the system as well as the scanner has excellent performance.

A stick-separation-slip method for sample micropositioning has been presented. By introducing a pulsed voltage into the stick-slip approach, the sample motion can be accomplished with high reliability even if the sawtooth waveform voltages are used. The mechanism of the method is briefly discussed and preliminary experiments have been performed. The relationship between the average step length of the sample movement and the driving voltage are measured at different pulsed voltages. The results show that under the condition of the pulsed voltage being 2.5 V, reliable movement with the step length from  $\sim 700$  nm to  $9$   $\mu\text{m}$  has been achieved.

Both scanning and micropositioning are important techniques in SPM. The work would provide an alternative way for SPM design and applications.

## ACKNOWLEDGMENTS

This work was supported by the National Natural Science Foundation of China (NSFC) No. 10827403 and the National 973 Project No. 2007CB936503.

- G. Binnig, H. Rohrer, C. Gerber, and E. Weibel, *Phys. Rev. Lett.* **49**, 57 (1982).
- G. Binnig, C. F. Quate, and C. Gerber, *Phys. Rev. Lett.* **56**, 930 (1986).
- L. Novotny and S. J. Stranick, *Annu. Rev. Phys. Chem.* **57**, 303 (2006).
- D. Croft, S. Stilson, and S. Devasia, *Nanotechnology* **10**, 201 (1999).
- I. A. Mahmood and S. O. R. Moheimani, *Nanotechnology* **20**, 365503 (2009).
- C. Bai, *Scanning Tunneling Microscopy and Its Application*, 2nd ed. (Springer-Verlag, New York, 2000).
- G. Binnig and D. P. E. Smith, *Rev. Sci. Instrum.* **57**, 1688 (1986).
- S. O. R. Moheimani, *Rev. Sci. Instrum.* **79**, 071101 (2008).
- K. Lieberman, N. Ben-Ami, and A. Lewis, *Rev. Sci. Instrum.* **67**, 3567 (1996).
- C. J. Chen, *Introduction to Scanning Tunneling Microscopy* (Oxford University Press, New York, 1993).
- D. W. Pohl, *Rev. Sci. Instrum.* **58**, 54 (1986).
- P. Niedermann, R. Emch, and P. Descouts, *Rev. Sci. Instrum.* **59**, 368 (1988).
- L. Libioulle, A. Ronda, I. Derycke, J. P. Vigneron, and J. M. Gilles, *Rev. Sci. Instrum.* **64**, 1489 (1993).
- R. Erlandsson and L. Olsson, *Rev. Sci. Instrum.* **67**, 1472 (1996).
- G. Shang, X. Qiu, C. Wang, and C. Bai, *Rev. Sci. Instrum.* **68**, 3803 (1997).
- C. Meyer, O. Sqalli, H. Lorenz, and K. Karrai, *Rev. Sci. Instrum.* **76**, 063706 (2005).
- A. Z. Stieg, P. Wilkinson, and J. K. Gimzewski, *Rev. Sci. Instrum.* **78**, 036110 (2007).
- S. H. Chang and S. S. Li, *Rev. Sci. Instrum.* **70**, 2776 (1999).
- S. C. Kim and S. H. Kim, *Mechatronics* **11**, 969 (2001).
- S. H. Chao, J. L. Garbini, W. M. Dougherty, and J. A. Sidles, *Rev. Sci. Instrum.* **77**, 063710 (2006).
- G. Y. Shang, C. Wang, J. Wu, C. L. Bai, and F. H. Lei, *Rev. Sci. Instrum.* **72**, 2344 (2001).
- R. Nowakowski, P. Luckham, and P. Winlove, *Biochim. Biophys. Acta* **1514**, 170 (2001).
- A. Touhami, A. Othmane, O. Ouerghi, H. Ben Ouada, C. Fretigny, and N. Jaffrezic-Renault, *Biomol. Eng.* **19**, 189 (2002).